

## Experimental study on the performance of a solar-biomass hybrid air-conditioning system

Boonrit Prasartkaew<sup>a,\*</sup>, S. Kumar<sup>b,1</sup>

<sup>a</sup> Department of Mechanical Engineering, Faculty of Engineering, Rajamangala University of Technology Thunyaburi, Klong 6, Thunyaburi, Pathumthani 12110, Thailand  
<sup>b</sup> Energy Field of Study, Asian Institute of Technology, P.O. Box 4, Klong Luang, Pathumthani 12120, Thailand

### ARTICLE INFO

**Article history:**  
 Received 4 March 2012  
 Accepted 7 January 2013  
 Available online

**Keywords:**  
 Solar cooling  
 Biomass gasifier  
 Hybrid thermal system  
 Air conditioning  
 Absorption chiller

### ABSTRACT

Renewable energy based technologies can be introduced for building cooling applications. Most studies on solar absorption cooling use fossil energy based auxiliary heaters. This paper presents experimental studies of a solar-biomass hybrid air conditioning system. The system performances at quasi-steady state conditions were analyzed. The results demonstrate that the system operates at about 75% of nominal capacity at an average overall system coefficient of performance of about 0.11. Performances of individual components of the system were also evaluated. The experimental results compared with results from other studies shows that the proposed system's performance in terms of chiller and overall system coefficient of performance is superior.

© 2013 Elsevier Ltd. All rights reserved.

### 1. Introduction

About 85% of the world's energy consumption is derived from the burning/combustion of fossil fuels as primary energy. In tropical countries, more than one third of the total electrical energy generated is consumed in commercial/residential buildings [1,2], and 70% of residential building energy consumption is used by air conditioning systems [3]. These are primarily by vapor compression systems. The use of renewable energy is one energy source option for such air conditioning system. The utilization of solar energy and biomass energy (through biomass gasification) is, therefore, a win-win solution.

Absorption chillers can be a key component in a building cooling system. They can be energized directly by the medium-temperature thermal energy from various sources with environmental friendly refrigerant. Most solar-powered absorption cooling projects to-date have utilized single-effect systems with low-temperature solar collectors [4]. From an energy saving point of view, a solar cooling system can save electrical energy in the range 25–40% when compared to an equivalent cooling capacity of a conventional water cooled refrigeration system [5].

The solar air conditioning system is attractive because the cooling load is roughly in phase with solar energy availability and it

can use an environmental friendly refrigerant. Since solar energy is intermittent, such systems cannot be continuously used (especially at night), and so an auxiliary heat source becomes inevitable. There are few experimental studies on solar cooling system without auxiliary heat source [6,7], and most systems use auxiliary/backup of fossil fuel, e.g. electricity, gas, and oil [8–12]. So, these systems are still fossil energy based cooling systems. To make the conventional solar cooling system to be a fully renewable energy cooling system, a fully solar-biomass hybrid air conditioning system (SBAC) was proposed [13]. Their theoretical study results show that the solar cooling system with biomass energy as an auxiliary/backup heater is promising. As a follow up, experimental studies were conducted to practically ascertain the working of such a system.

This paper presents details of a SBAC system design and the performance investigation of a SBAC with details of the experimental set up, performance of individual components and the complete system. Section 2 describes the proposed system design. Section 3 presents the details of system description. Section 4 presents the experimental procedure. Section 5 reports the experimental results and discussion. Section 6 presents a comparison with other studies. The conclusion of the study is presented in Section 7.

### 2. System design

The first step in the design of a cooling system is the estimation of cooling load of the conditioned space. The maximum cooling load is about 4.5 kW or 1.3 tons of refrigeration (TR) and occurs at

\* Corresponding author. Tel.: +66 8 9767 2533; fax: +66 2 549 3432.  
 E-mail addresses: [prasartkaew@yahoo.com](mailto:prasartkaew@yahoo.com) (B. Prasartkaew), [kumar@ait.ac.th](mailto:kumar@ait.ac.th) (S. Kumar).  
<sup>1</sup> Tel.: +66 2 524 5403; fax: +66 2 524 5439.

Nomenclature			
$A$	area ( $m^2$ )	ge	generator
$C_p$	water specific heat capacity ( $kJ/kg.K$ )	i	inlet
$F_R(\tau\alpha)$	intercept efficiency (-)	o	outlet
$F_R U_L$	collector heat loss efficiency coefficient ( $W/m^2K$ )	set	set point value
$H$	solar radiation on tilted surface ( $kW/m^2$ )	t	storage tank
$\dot{m}$	mass flow rate ( $kg/s$ )	tl	tank to load
$\dot{Q}$	heat rate ( $kW$ )	u	useful energy
$T$	temperature ( $^{\circ}C$ )	<b>Acronyms</b>	
UA	overall heat loss coefficient ( $W/K$ )	B	biomass steady state condition
V	volume ( $m^3$ )	BGB	biomass gasifier-boiler
<b>Greek symbols</b>		BM	biomass
$\eta$	efficiency	COP	coefficient of performance
<b>Subscripts</b>		COP <sub>sys</sub>	overall system coefficient of performance
b	boiler	FCU	fan coil unit
bl	boiler to load	S	solar steady state condition
c	collector	SBAC	solar-biomass hybrid air conditioning system
ev	evaporator	SCR	solar to cooling ratio
		SF	solar fraction
		SWH	solar water heating system

around 16:00–17:00. For the prescribed cooling load, the model described in Ref. [13] was used for component or sub-system sizing which will thus form the complete system. The model was developed using the following assumptions:

- (1) The model considered the energy and mass balances at each component, and of the overall system.
- (2) The system is considered to be at steady state
- (3) The specific heat and density of the working fluids are constant.
- (4) The loss of the water vapor and moisture (at the hot water storage tank and solar collector vents) is not taken into account.
- (5) There is no pressure loss and no heat loss/gain in the lines (pipes) connecting the system components.
- (6) The fluid temperatures increasing due to the friction in plumbing and valves, blowers and pumps are negligible.
- (7) The energy considered is solar and biomass energy, while the power consumed by other equipment (e.g. pumps, blower, fans and controllers) is excluded.

The input parameters of each component are the specification data provided by the manufacturer or obtained from the individual component tests. The model comprises of the governing equations for each sub system, and that the inputs and outputs between each sub-system were according to the system configuration. Fig. 1 summarizes the input and output parameters of the simulation. Table 1 shows the system specifications used in this study. In the system configuration selection and system design, the input parameters were varied to obtain the maximum system performance. The sizes of solar water heating (SWH) sub-system and auxiliary heating sub-system depend on the (prescribed) solar fraction (or solar to auxiliary heat ratio, SF). The weather data used was the metrological condition of Bangkok, Thailand (Asian Institute of Technology) with the SF value of 0.7.

### 3. Description of the proposed system

Fig. 2 shows the schematic diagram of the solar-biomass hybrid absorption cooling system. It consists of three main components (sub-systems): solar water heating system with storage tank, biomass gasifier-boiler (BGB) system, and (single-effect) absorption chiller.

The solar energy absorbed by the SWH system heats the water, which is then pumped to a storage tank. The BGB system is located between hot water storage tank and absorption chiller. This component works as auxiliary boiler when solar energy is not sufficient and as the main heat source when solar radiation is not available. The gasifier boiler is controlled by controller and supplies hot water to the chiller. The cooling is provided by a single-effect lithium bromide (LiBr)-water absorption chiller. The heat required for its generator is drawn from hot water pumped from a storage tank fed by the solar collectors and/or sometimes boosted/fed by biomass boiler. The condenser and absorber of the chiller are cooled by cooling water pumped through a cooling tower. The chilled water produced from the chiller is pumped to the fan coil unit in the room to provide comfort conditions.

The SBAC system was installed at the Asian Institute of Technology (AIT), Bangkok. This system consists of 26 flat plate collector field with total area of  $50 m^2$ , a 400 l hot water storage tank and a single-effect LiBr-water absorption chiller of 7 kW nominal capacity. Fig. 3 shows the photo of experimental system.

To study the performance of the SBAC system, temperatures, flow rates, electricity and solar insolation were measured. A data logger (Campbell Scientific Inc. model CR-10X) equipped with multiplexer (solid-state type AM25T) recorded temperatures with type-K thermocouples installed at different locations and solar insolation data were also measured at the meteorological station at every five-minute intervals. Other data (water flow rate and biomass consumption rate) were manually measured and recorded every half an hour.

### 4. Experimental procedure

Biomass (charcoal in the gasifier) and water levels (in boiler, storage tank and cooling tower) were checked, and the SWH and BGB system were started at around 8 am. To prevent the crystallization at the absorption chiller, it was started later when the boiler temperature was higher than  $70^{\circ}C$ . The controller switches the BGB depending on average tank temperature. When the BGB is switched on, the hot water temperature was controlled at the set point temperature of  $84^{\circ}C$ , which is the optimum temperature for the chiller. When the temperature difference between the collector outlet and average tank temperature was less than  $1^{\circ}C$ , the

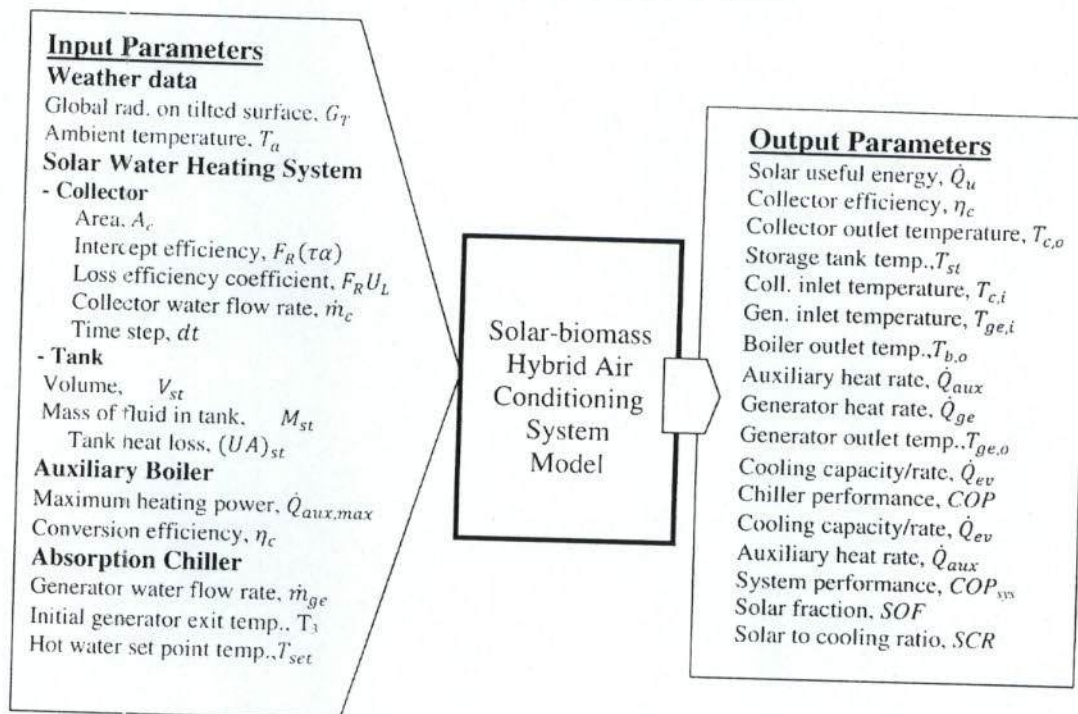


Fig. 1. The inputs and outputs of the mathematical model.

collector pump was switched off and switched on again when this temperature difference was higher than 2 °C. The water flow rate of collector, generator, cooling tower and chilled water pumps were set at 1200, 1500, 5400 and 900 kg/hr, respectively. At the end of experimental day, the overall system was turned off when the gasifier cannot produce any producer gas (in an actual system, the charcoal was continuously loaded and ash was removed) at around 6 pm.

The quasi-steady state condition for each experimental result was defined with the criteria that all variation between time steps

of each measured parameters is less than 10% over a period of 30 min or longer. The data during the quasi-steady state conditions was chosen and used for the performance analysis, and 5 min measurement records were used to ascertain these conditions.

## 5. Results and discussion

Experiments were conducted to study the performance of the system components and overall system of SBAC system. The theoretical study results reported in Ref. [13] showed that the lowest performance of SBAC system: e.g.: lowest solar fraction, highest biomass consumption and lowest  $COP_{sys}$ , are during the rainy season. To demonstrate as the ultimate weak system performance, the experimental system was tested during rainy season period (3–30 September 2010). Complete data of 11 days were chosen for the analysis.

### 5.1. Sky condition and biomass consumption

The solar radiation during the experiments is presented in Table 2. The solar radiation incidence on the collector ranged between 11.25 and 18.81 MJ/m<sup>2</sup>.day. This period included all the three sky conditions: partly cloudy, cloudy and very cloudy with the average solar insolation of 17.3, 14 and 11.3 MJ/m<sup>2</sup>.day, respectively. The results show that average biomass consumption during this period is about 15 kg a day.

### 5.2. Performance analysis

Two types of quasi-steady state period depend on an energizing source: solar (called 'solar quasi-steady state period') and biomass (called 'biomass quasi-steady state period') periods. To demonstrate the energy balance and system performance analysis, the experimental results on 16 September 2010 were used. The

Table 1  
System specifications used in this study.

Component	Items	Value	Unit
<i>Solar water heating system</i>			
Collector	Area, $A_c$	54	m <sup>2</sup>
	Intercept efficiency, $F_R(\tau\alpha)$	0.789	–
	Loss efficiency coefficient, $F_R U_L$	5.829	W/m <sup>2</sup> K
	Collector flow rate, $\dot{m}_c$	1200	kg/hr
Tank	Volume, $V_t$	1	m <sup>3</sup>
	Tank heat loss coefficient, $(UA)_t$	4.068	W/K
	Hot water set temperature, $T_{set}$	84	°C
Auxiliary Boiler	Maximum heating power	15	kW
<i>Absorption Chiller (at nominal condition)</i>			
Absorption Chiller	Absorption chiller nominal size	7	kW
	Chilled water outlet temperature	9	°C
	Chilled water inlet temperature	14	°C
	Chilled water circulation flow rate	0.333	l/s
	Generator input	11.6	kW
	Generator inlet temperature range	75–100	°C
	Generator circulation flow rate	0.463	l/s
	Cooling water inlet temperature	29.5	°C
	Cooling water outlet temperature	34.5	°C
	Cooling water circulation volume	0.888	l/s
	Weak (dilute) solution mass fraction	54	%
	Strong solution mass fraction	59	%

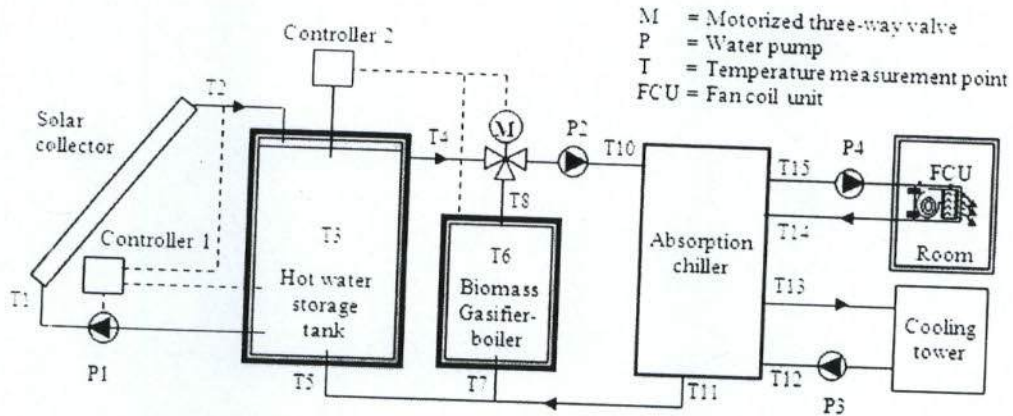


Fig. 2. Schematic diagram of the solar-biomass hybrid absorption cooling system.

performance is described using quasi-steady state data as shown in Fig. 4. There are 3 quasi-steady state periods: two solar quasi-steady state periods, S1 (11:25 to 12:10) and S2 (13:10 to 14:10), and one biomass quasi-steady state period, B3 (15:50 to 17:10).

5.2.1. Solar collector

Fig. 5 shows the water temperature at collector inlet and outlet. The water outlet temperature began to rise rapidly after the collector circulation pump was activated at 8:30 am. Consequently, the storage tank temperature also increased. The maximum temperature difference between the collector inlet and outlet during quasi-steady state at sunshine period (S2) was 10 °C. During the solar quasi-steady state period, the maximum and average water temperatures at collector outlet were 94 and 93.4 °C, respectively.

During solar quasi-steady state condition (S1), the average collector efficiency is about 32%. The collector efficiency calculated every 5 min by Eq. (1) is shown in Fig. 6. During the solar quasi-steady state conditions (S1) and (S2), the collector efficiency varied in the range 27–39%.

$$\eta_c = \dot{Q}_u / (G_T A_c) \tag{1}$$

where,

$$\dot{Q}_u = \dot{m}_c C_p (T_{c,o} - T_{c,i}) \tag{2}$$

5.2.2. Storage tank

Fig. 7 shows the average storage tank temperature and temperatures at its outlet and inlet. Heat will be removed from the tank whenever the hot water was drawn from the top of the tank through the motorized 3-way valve. From 10:45 to 15:20 (4.75 h), when the average tank temperature reached 83 °C and until it was reduced to 80 °C, the chiller generator was energized with heat from the tank.

To determine the efficiency of the hot water storage tank, the ratio of energy supplied to load to energy input from collector was calculated using Eq. (3) and the results are shown in Fig. 8.

$$\eta_t = \dot{Q}_{dl} / \dot{Q}_u \tag{3}$$

where,

$$\dot{Q}_{dl} = \dot{m}_{ge} C_p (T_{t,o} - T_{t,i}) \tag{4}$$

The results shown that, during quasi-steady state condition (S2), the hot water storage tank efficiency varied in the range 64–99%.

5.2.3. Biomass gasifier-boiler

Using the lower heating value of biomass, LHV<sub>BM</sub> = 25.7 MJ/kg, the average biomass consumption rate, ( $\dot{m}_{BM}$ ) was determined from:

$$\dot{m}_{BM} = \frac{\text{Total amount of biomass used per day [kg]}}{\text{Total BGB operating time in a day [s]}} \tag{5}$$

For this experimental day, the total of BGB operating time is the summation of the time periods of BI, BII and BIII (as shown in Fig. 4).

Table 2  
Sky condition and test mode of each experimental day.

Day no.	Date D-M-Y (day no. of year)	H [MJ/m <sup>2</sup> .day]	Sky condition	Biomass consumed [kg]
1	4-09-10 (247)	14.60	Cloudy	19.8
2	5-09-10 (248)	18.29	Partly cloudy	20.2
3	9-09-10 (252)	11.25	Very cloudy	18.3
4	12-09-10 (255)	16.32	Partly cloudy	15.4
5	14-09-10 (257)	13.40	Cloudy	15.3
6	15-09-10 (258)	16.60	Partly cloudy	13.1
7	16-09-10 (259)	18.81	Partly cloudy	14.8
8	17-09-10 (260)	16.31	Partly cloudy	13.7
9	19-09-10 (262)	11.31	Very cloudy	11.4
10	23-09-10 (266)	14.80	Cloudy	10.1
11	24-09-10 (267)	13.02	Cloudy	13.9

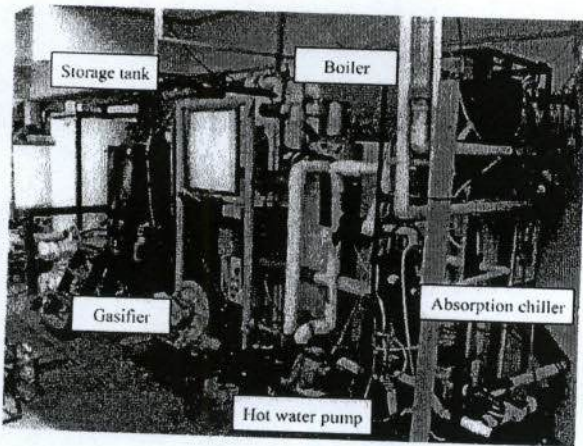


Fig. 3. Experimental system installed at the Asian Institute of Technology.

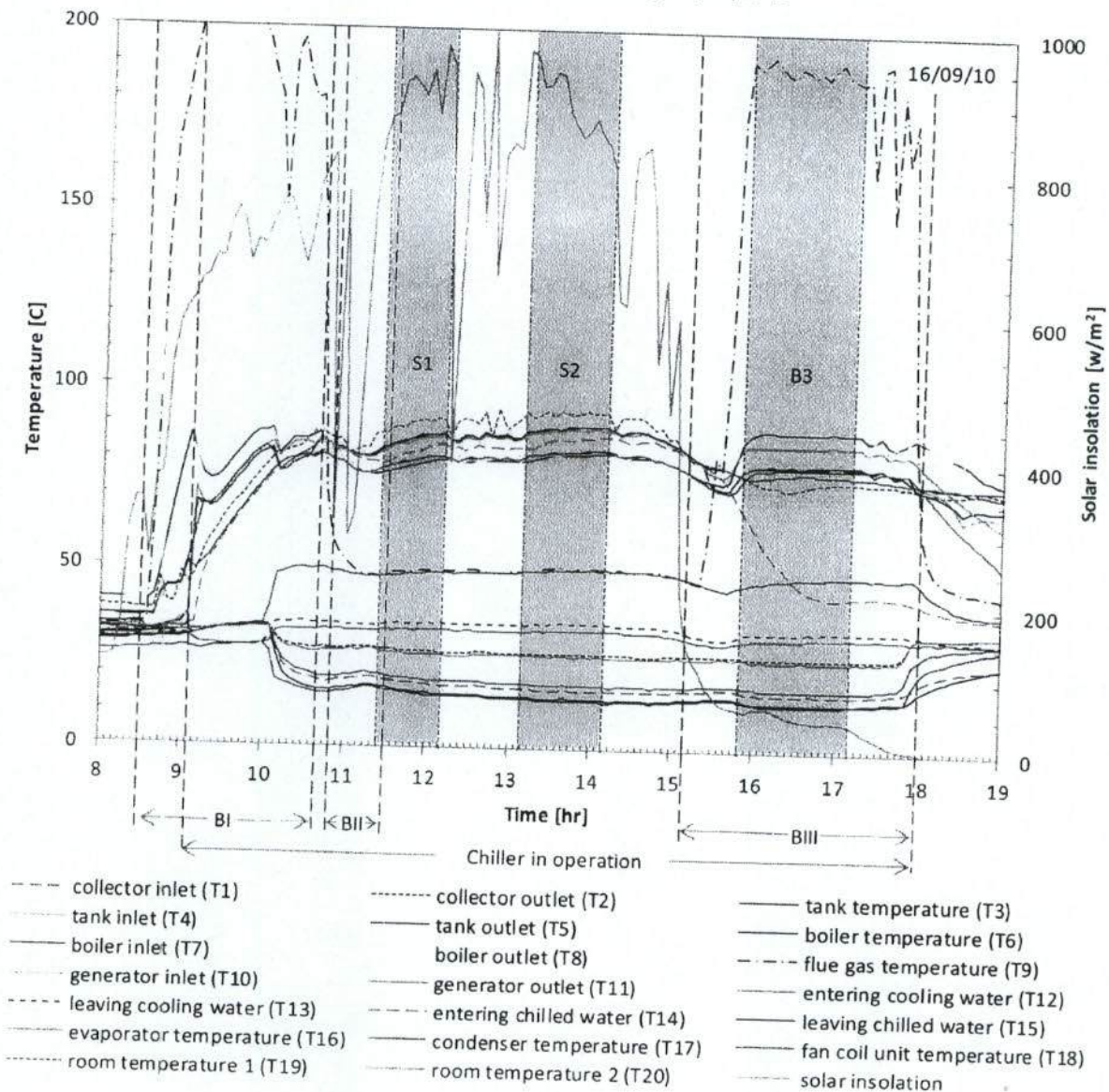


Fig. 4. Quasi-steady state periods on September 16, 2010.

Fig. 9 shows the temperature profiles of water in boiler inlet and outlet. It can be seen that during the biomass quasi-steady state condition (B3), the temperature difference between boiler inlet and outlet temperatures is about 8 °C. The total amount of biomass (charcoal) consumed was about 14.8 kg for this experimental day.

The overall energy conversion efficiency of the BGB is defined by Eq. (6).

$$\eta_{BGB} = \dot{Q}_{bl} / (\dot{m}_{BM} LHV_{BM}) \quad (6)$$

where,

$$\dot{Q}_{bl} = \dot{m}_{ge} C_p (T_{b,o} - T_{b,i}) \quad (7)$$

The experimental results (as shown in Fig. 10) show that during quasi-steady state condition (B3), the overall efficiency of the BGB system varied in the range 63–77%.

#### 5.2.4. Absorption chiller

Fig. 11 shows a plot of the absorption chiller temperatures. When the chiller generator was activated by water from boiler at 10:10, the evaporator temperature started decreasing. The chilled water temperature reached 13 °C at 16:20 when the chiller was energized by the BGB.

With the input and output energies, the chiller coefficient of performance can be estimated using Eq. (8). The calculation results show that the chiller coefficient of performance during the operation on solar energy was little lower than the operation on biomass energy (Fig. 12) with the values of 0.50 and 0.53, respectively.

$$COP = \dot{Q}_{ev} / \dot{Q}_{ge} \quad (8)$$

#### 5.2.5. Overall system performance

As shown in Fig. 12, the coefficient of performances of the chiller (COP) and overall system (COP<sub>sys</sub>) during experimental day, calculated using Eqs. (8) and (9), respectively. The daily performance

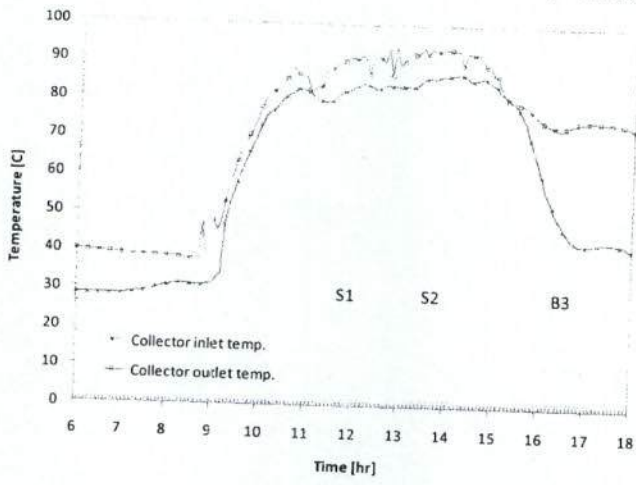


Fig. 5. Collector inlet and outlet temperature profiles.

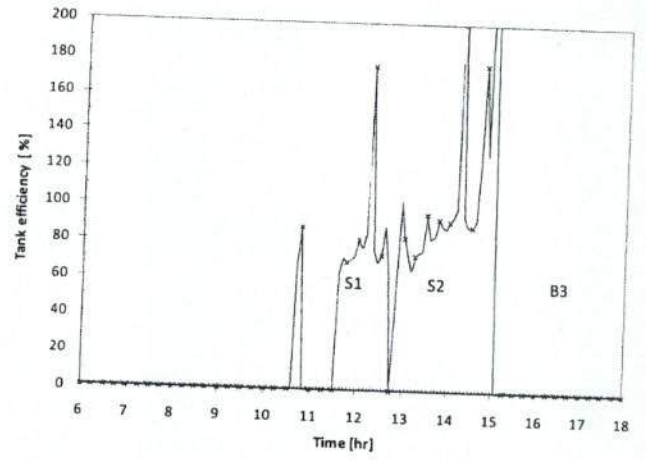


Fig. 8. Hot water storage tank efficiency.

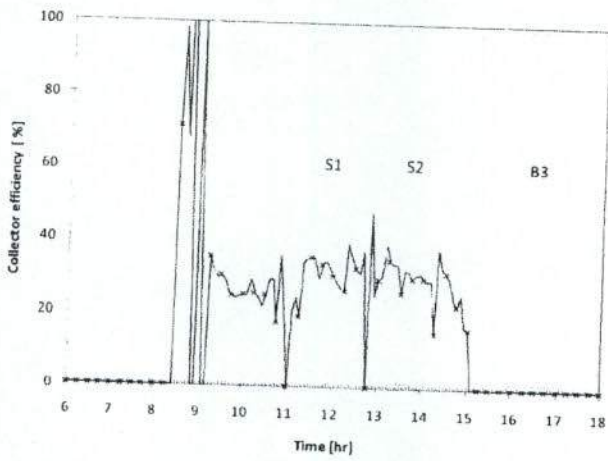


Fig. 6. Collector efficiency.

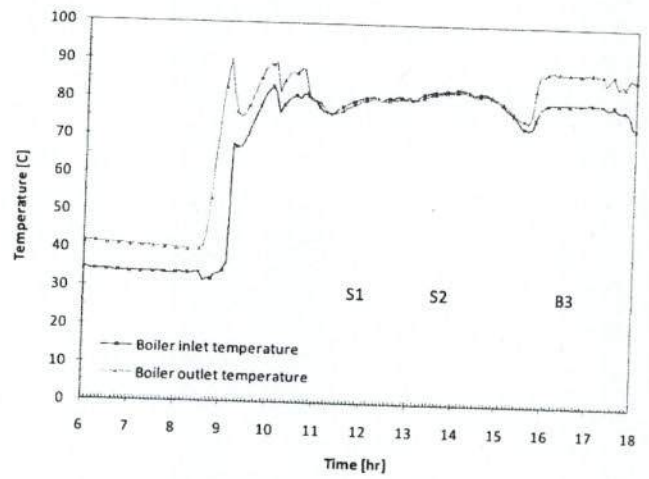


Fig. 9. Boiler inlet and outlet temperature profiles.

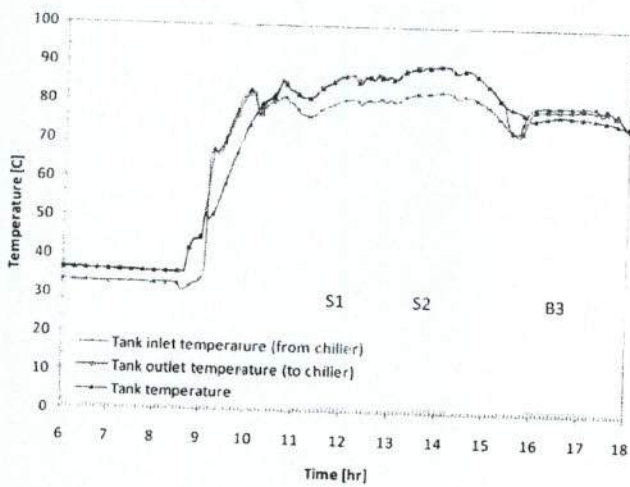


Fig. 7. Storage tank temperature profiles.

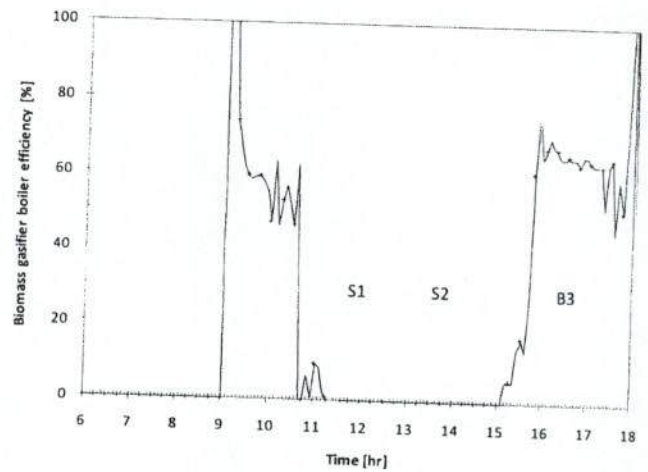


Fig. 10. Biomass gasifier-boiler efficiency.

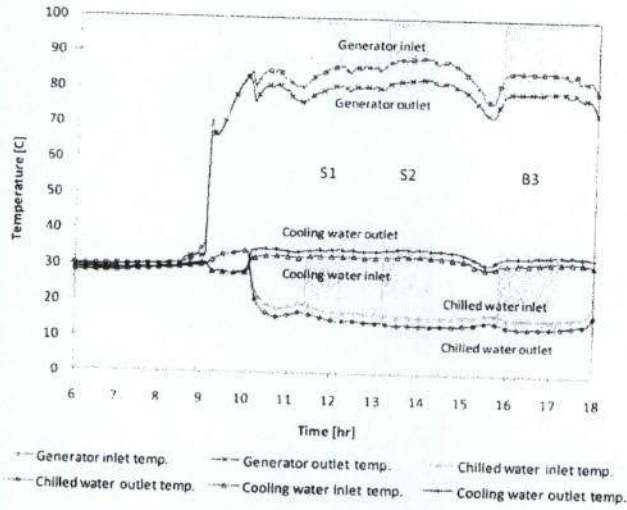


Fig. 11. Absorption chiller temperature profiles.

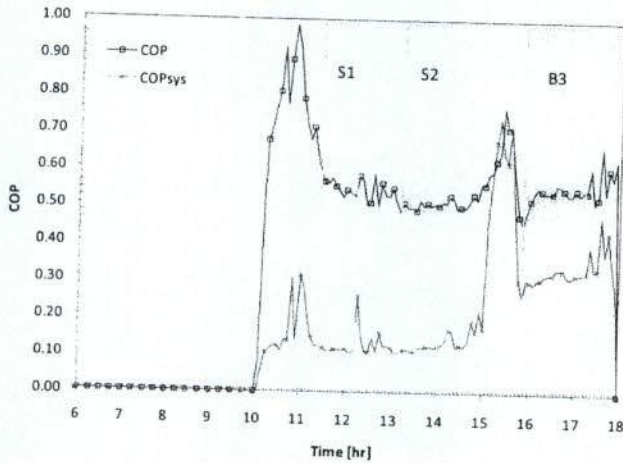


Fig. 12. Chiller and overall system coefficient of performances.

parameters of all experiments are summarized in Table 3. Since the chilled water was produced at around 10:10, both COP and  $COP_{sys}$  values were higher than zero at this time. During quasi-steady state conditions (S1 and S2 and B3), the COP and  $COP_{sys}$  varied in the range 0.45–0.64 (with daily average of 0.67) and 0.15 to 0.33 (with daily average of 0.1), respectively with the average of 0.53 and 0.18, respectively.

**Table 3**  
Experimental results of 11 experimental days.

Day no.	Solar insolation [MJ/day]	Biomass energy [MJ/day]	Daily average $\eta_c$ [-]	Daily average COP [-]	Daily average $COP_{sys}$ [-]	Daily average SCR [-]	Daily average SF [%]
1	715.23	508.86	0.14	0.77	0.10	0.17	58.43
2	896.37	519.14	0.17	0.81	0.10	0.16	63.32
3	551.29	470.31	0.14	0.65	0.09	0.16	53.96
4	799.73	395.78	0.23	0.81	0.11	0.17	66.89
5	656.68	393.21	0.14	0.70	0.10	0.16	62.55
6	813.17	360.25	0.25	0.51	0.11	0.15	69.30
7	921.92	380.36	0.28	0.55	0.11	0.16	70.79
8	799.10	352.09	0.27	0.53	0.10	0.15	69.42
9	554.14	292.98	0.17	0.54	0.12	0.18	65.41
10	725.33	259.57	0.25	0.64	0.10	0.14	73.65
11	637.98	357.23	0.13	0.83	0.10	0.16	64.10
<b>Average</b>	<b>733.72</b>	<b>389.98</b>	<b>0.20</b>	<b>0.67</b>	<b>0.10</b>	<b>0.16</b>	<b>65.26</b>

**Table 4**  
Comparison of experimental results between the current study and literature.

Parameters	Current study	Li and Sumathy [14]	Syed et al. [6]	Hidalgo et al. [7]	Monné et al. [15]
Collector type, area [m <sup>2</sup> ]	Flat plate, 50	Flat plate, 38	Flat plate, 49.9	Flat plate, 50	Flat plate, 37.5
Nominal cooling capacity	7 kW (nominal)	4.7 kW (rated)	35 kW	NA	4.5
Tank volume [m <sup>3</sup> ]	0.4	2.75	2	2	Not used
Tank volume ratio [m <sup>3</sup> /m <sup>2</sup> ]	8	72	40	40	–
Auxiliary heater	Yes	Yes	NO	NO	NA
COP	0.54 (steady state), 0.67 (average)	~0.55 (read from graph)	0.42 (daily average)	0.33 (season average)	0.46 –0.56
$COP_{sys}$	0.31 (steady state), 0.11 (daily average)	0.07 (partitioned tank)	0.11 (daily average)	0.07 (season average)	NA
Solar fraction (%)	70.8 (daily average)	NA	100 (no aux. heater)	100 (no aux. heater)	NA

$$COP_{sys} = \dot{Q}_{ev} / (C_T A_c + \dot{m}_{BM} LHV_{BM}) \quad (9)$$

## 6. Comparison of results

A comparison of the experimental parameters and performance obtained from this study and those obtained from the literature (as shown in Table 4) are discussed in this section. To compare the performance, other studies, which have comparable chiller and collector type and size and configuration, were taken into account.

Based on the available data of collector type, area and use for a small size chiller (smaller than 10 kW), the study of [14] is the most similar to the current study (all hot water loop can be mixed at the tank) while the others: [6,7,15], use the plate heat exchanger between collector and tank water. Syed et al. [6] and Rodriguez Hidalgo et al. [7] use 35 kW absorption chiller and [15] use smaller chiller and collector area.

The comparison shows that with BGB as auxiliary heat source, the proposed system outperforms others, in both COP and  $COP_{sys}$ .

## 7. Conclusion

The performance of a solar-biomass hybrid air conditioning system was evaluated in this study. The experimental system was tested during rainy season period and 11 days with complete data were chosen for this analysis. The experiments were started at around 8 am and stopped at around 6 pm. The experimental results show that a solar-biomass hybrid air conditioning system is promising. The results demonstrate that the system operated at about 75% of nominal capacity and an average overall system coefficient of performance of about 0.11 was achieved. The results also show that, due to the limitation of heat absorption at the evaporator of this (small size) chiller, the supplied excess heat was rejected at the cooling tower. The biomass-gasifier boiler system, used as a booster/auxiliary heater, can improve the overall system performance. Comparison of performance of solar cooling system with different auxiliary heat sources shows that the proposed system outperforms the others, in terms of chiller and overall system coefficient of performance.

## References

- [1] NRCT. Foresight research 2008. Office of the National Research Council of Thailand; 2008.
- [2] Shaahid SM, Elhadidy MA. Economic analysis of hybrid photovoltaic diesel battery power systems for residential loads in hot regions-A step to clean future. *Renewable and Sustainable Energy Reviews* 2008;12:488–503.
- [3] Vangtook P, Chirarattananon S. Application of radiant cooling as a passive cooling option in hot humid climate. *Building and Environment* 2007;42(2): 543–56.
- [4] Balaras CA, Grossman G, Henning HM, Ferreira CAI, Podesser E, Wang L, et al. Solar air conditioning in Europe—an overview. *Renewable and Sustainable Energy Reviews* 2007;11:299–314.
- [5] Afonso C. Recent advances in building air conditioning systems. *Applied Thermal Engineering* 2006;26:1961–71.
- [6] Syed A, Izquierdo M, Rodriguez P, Maidment G, Missenden J, Lecuona A, et al. A novel experimental investigation of a solar cooling system in Madrid. *International Journal of Refrigeration* 2005;28:859–71.
- [7] Rodriguez Hidalgo MC, Rodriguez Aumente P, Izquierdo Millan M, Lecuona Neumann A, Salgado Mangual R. Energy and carbon emission savings in Spanish housing air-conditioning using solar driven absorption system. *Applied Thermal Engineering* 2008;28:1734–44.
- [8] Qu Ming, Yin Hongxi, Archer David H. A solar thermal cooling and heating system for a building: experimental and model based performance analysis and design. *Solar Energy* 2010;84:166–82.
- [9] Perez de Vinaspre M, Bourouis M, Coronas A, Garcia A, Soto V, Pinazo JM. Monitoring and analysis of an absorption air-conditioning system. *Energy and Buildings* 2004;36:933–43.
- [10] Ali Ahmed Hamza H, Noeres Peter, Pollerberg Clemens. Performance assessment of an integrated free cooling and solar powered single-effect lithium-bromide-water absorption chiller. *Solar Energy* 2008;82:1021–30.
- [11] Pongtornkulpanich A, Thepa S, Amornkitbamrung M, Butcher C. Experience with fully operational solar-driven 10-ton H<sub>2</sub>O/LiBr single-effect absorption cooling system in Thailand. *Renewable Energy* 2008;33:943–9.
- [12] Sumathy K, Huang ZC, Li ZF. Solar absorption cooling with low grade heat source – a strategy of development in South China. *Solar Energy* 2002;72(2): 155–65.
- [13] Prasartkaew Boonrit, Kumar S. A low carbon cooling system using renewable energy resources and technologies. *Energy and Buildings* 2010;42: 1453–62.
- [14] Li ZF, Sumathy K. Experimental studies on a solar powered air conditioning system with partitioned hot water storage tank. *Solar Energy* 2001;71(5): 285–97.
- [15] Monné C, Alonso S, Palacín F, Serra L. Monitoring and simulation of an existing solar powered absorption cooling system in Zaragoza (Spain). *Applied Thermal Engineering* 2011;31:28–35.